

Grain Boundaries in Gallium Arsenide Nanocrystals Under Pressure: A Parallel Molecular-Dynamics Study

Sanjay Kodiyalam, Rajiv K. Kalia, Hideaki Kikuchi, Aiichiro Nakano, Fuyuki Shimojo, and Priya Vashishta
*Concurrent Computing Laboratory for Materials Simulations, Department of Physics & Astronomy
and Department of Computer Science, Louisiana State University, Baton Rouge, Louisiana 70803-4001*
(Received 18 September 2000)

Structural transformation in gallium arsenide nanocrystals under pressure is studied using molecular-dynamics simulations on parallel computers. It is found that the transformation from fourfold to sixfold coordination is nucleated on the nanocrystal surface and proceeds inwards with increasing pressure. Inequivalent nucleation of the high-pressure phase at different sites leads to inhomogeneous deformation of the nanocrystal. This results in the transformed nanocrystal having grains of different orientations separated by grain boundaries. A new method based on microscopic transition paths is introduced to uniquely characterize grains and deformations.

DOI: 10.1103/PhysRevLett.86.55

PACS numbers: 36.40.Ei, 61.50.Ks, 81.30.Hd

Structural phase transitions in semiconductors under pressure is a subject of considerable experimental and theoretical research activity. Experimentally, bulk gallium arsenide (GaAs) has been found to undergo a transformation from the fourfold coordinated zinc blende structure to a sixfold coordinated orthorhombic structure at a pressure of 17 GPa [1,2]. Total-energy calculations support this observation [3–5]. Pioneering high-pressure experiments on semiconductor nanocrystals [6–8] have been carried out by Alivisatos and co-workers to investigate the effect of finite size on the solid-solid phase transformation and to explore the possibility of stabilizing bonding geometries that are different from the corresponding bulk. In these experiments, the elevated transition pressure of the nanocrystals as compared to the bulk has been attributed to surface energy effects with the nanocrystals changing shape coherently by undergoing uniform deformation during the transformation [7,8].

The microscopic mechanism of the structural transformation in nanocrystals is, however, not completely understood [9] and atomistic simulations are expected to play an important role in elucidating these mechanisms. For example, *ab initio* molecular dynamics (MD) has been used in theoretical investigations of high-pressure structural transformations in silica [10,11]. Recently, this technique was used to study structural transformation of a silicon cluster that is embedded in a classical soft-sphere liquid that serves as a hydrostatic pressure medium [12]. The *ab initio* approach currently allows the simulation of a nanocrystal size of only ~ 30 atoms for a total simulation time ~ 10 ps. On the other hand, recent developments in reliable interatomic potentials have allowed, for the first time, classical MD simulations of both forward and reverse structural transformations under pressure in bulk silicon carbide (SiC) [13] and GaAs [14]. A new microscopic mechanism for the transformation has been identified. This encourages us to investigate similar pressure-driven transformations in single nanocrystals of GaAs using the MD approach. The nanocrystals are embedded

in a hydrostatic pressure medium for which we choose a Lennard-Jones (LJ) liquid. The MD implementation on parallel computers has allowed us to study large nanocrystals with ~ 5000 atoms embedded in $\sim 500\,000$ atoms of LJ liquid for total simulation times of ~ 200 ps.

The results show that in GaAs nanocrystals under pressure a transformation from the zinc blende phase to the rocksalt phase nucleates on the surface and proceeds inwards with increasing pressure. Inequivalent nucleation at different sites on the surface leads to spatially inhomogeneous deformations which results in the transformed nanocrystals having grains of the rocksalt phase separated by grain boundaries. Geometric considerations show that inhomogeneous deformation does not always lead to grain boundaries but can nevertheless be identified from the nonellipsoidal shape of the transformed nanocrystal.

Isothermal-isobaric [15–17] MD simulations are carried out by using an effective interatomic potential for GaAs that includes two- and three-body terms. In order to reproduce both the forward and reverse structural transformations of the bulk under pressure, it is essential that the three-body potential differ from the Stillinger-Weber form [14,18,19]. With this potential the calculated structure and nearest-neighbor distance during the pressure-induced phase transformation in the bulk and the photon density of states [14] and the static structure factor of amorphous GaAs [19] agree well with the experimental results [2,20,21]. The potential parameters of the LJ atoms are chosen such that at the operating simulation temperature there is a wide range of pressures for which this system remains in the liquid state [22]. The interaction between the LJ atoms and the atoms of the GaAs nanocrystal is chosen to be purely repulsive to prevent a LJ atom from entering the GaAs nanocrystal.

The initial configuration of the system is constructed by cutting a spherical nanocrystal of GaAs of diameter 60 \AA from the bulk (zinc blende structure) and placing it in a cavity in a fcc lattice of LJ atoms. This is accomplished by removing LJ atoms, in the region of the nanocrystal

and a surrounding skin region, from the fcc lattice. The initial density of the LJ lattice is chosen such that at the simulation temperature this subsystem is at its liquid and gas-liquid phase boundaries [22], where the pressure is 2.3 GPa. Beginning with such an initial configuration, the temperature of the system is increased by scaling velocities of atoms in a simulation at constant volume that is run for $\sim 10\,000$ time steps (MD time step = 2 fs). This initial procedure melts the lattice of LJ atoms into a liquid. All subsequent simulations are performed in the isothermal-isobaric ensemble. The system is thermalized at a pressure of 2.5 GPa for $\sim 10\,000$ time steps (Fig. 1). The pressure is then raised in steps 2.5–5 GPa at a rate of 2.5 GPa per 500 time steps. At each new value of pressure the system is thermalized for $\sim 5\,000$ time steps. This procedure is continued until the GaAs nanocrystal undergoes a structural transformation. Another simulation schedule in which the pressure is increased linearly at a rate of 2.5 GPa per 10 000 time steps is adopted when the structural transformation is monitored continuously.

For the nanocrystals in this study it is found that structural transformation nucleates at the surface and proceeds inwards with increasing pressure. This is illustrated in Fig. 2 in which the structure is analyzed by spatially resolving the bond angles into 10-Å-wide shells—with peaks at about 109° and 90° identifying the zinc blende and rocksalt structures, respectively. The shortest closed path of alternating Ga-As bonds, which is defined to be a ring [19,23], can also be used to distinguish the zinc blende and rocksalt phases. In the zinc blende structure

the rings are nonplanar and are 6-membered, while in the rocksalt structure they are planar and 4-membered. The cross section of the spherical nanocrystal (diameter = 60 \AA) at 17.5 GPa [Fig. 2(a)] shows such 4-membered rings corresponding to the rocksalt structure in the outer and middle shells, whereas the inner shell shows 6-membered rings corresponding to the untransformed zinc blende structure. Bond-angle distributions (average of the As-Ga-As and the Ga-As-Ga bond angles) corroborate this result [Fig. 2(b)]—with the outer shell having a peak about 90° while the inner shell continues to show zinc blende structure with a peak about 109° . At a pressure of 22.5 GPa the structural transformation of this nanocrystal is completed, since 4-membered rings are observed in the innermost shell [Fig. 2(c)] and the bond-angle distribution corresponding to all of the shells shows a peak about 90° [Fig. 2(d)]. From the evolution of the ring structure and the bond angles, it is inferred that the structural transformation nucleates at the surface and progresses inwards with increasing pressure.

Two distinct grains of the rocksalt phase with inequivalent orientation can be seen in Fig. 2(a). The origin of the inequivalence can be understood in terms of the different paths for structural transformation. Figure 3 schematically illustrates one such transformation path. In analogy with MD simulations of similar transformations in bulk SiC [13] and GaAs [14], it is found here that the transformation proceeds without breaking any existing bonds and with the

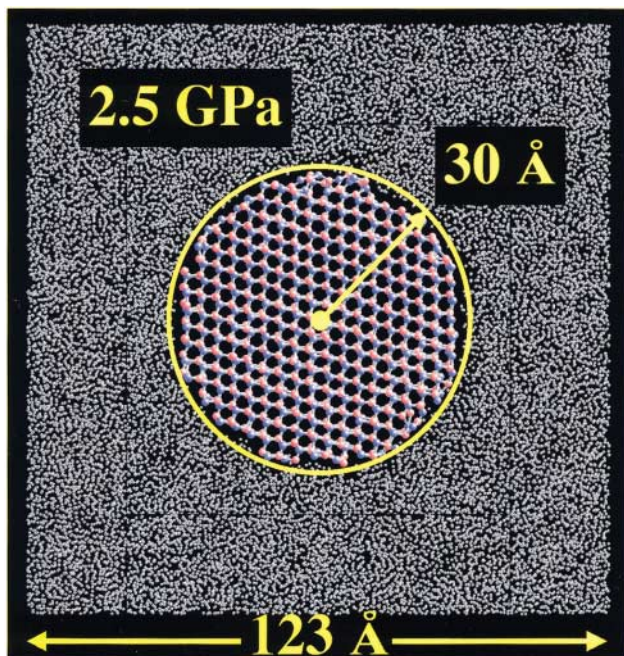


FIG. 1 (color). Initial thermalized system. The GaAs nanocrystal is embedded in the Lennard-Jones liquid that serves as a hydrostatic pressure medium.

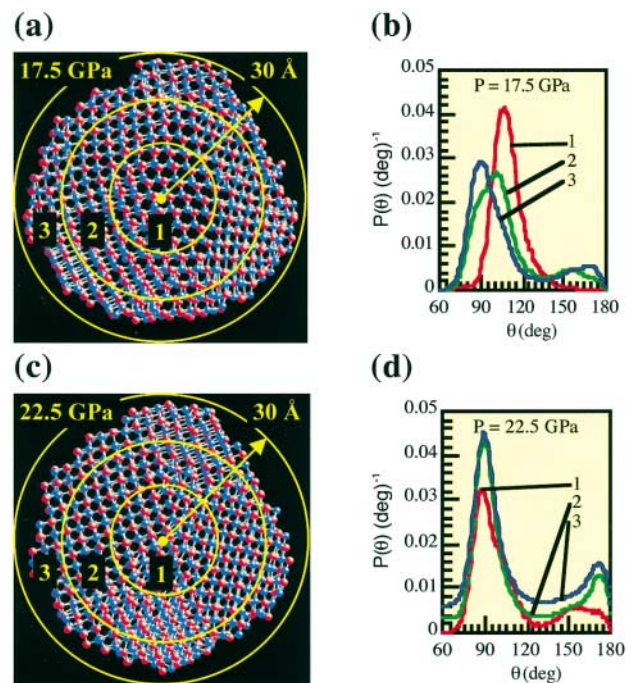


FIG. 2 (color). Structural transformation in a GaAs nanocrystal from outer to inner shells. 8 Å slice of the spherical nanocrystal of diameter 60 \AA at a pressure of 17.5 GPa (a) and at 22.5 GPa (c). Bond-angle distributions at 17.5 GPa (b) and at 22.5 GPa (d).

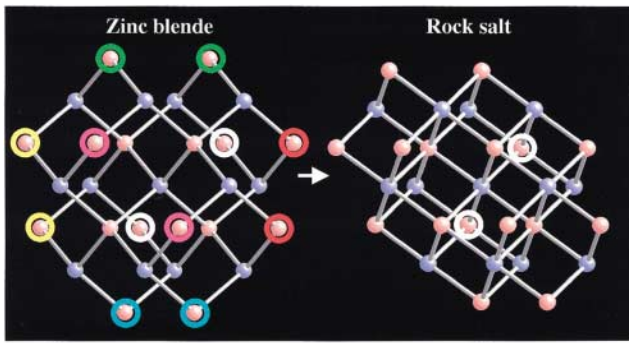


FIG. 3 (color). Paths for structural transformation in the GaAs nanocrystal. The paths for structural transformation from the zinc blende to rocksalt phases are illustrated by pairs of As atoms that can bond to the centrally located Ga atom. Any pair of these next-nearest-neighbor As atoms are at a distance of 0.75 lattice constants along one of the conventional fcc unit cell vectors. The six possibilities are indicated by the distinct pairs (each shown circled by a different color) of As atoms. The path in which the Ga atom bonds to As atoms identified by white circles leads to the rocksalt structure shown. Each of these paths corresponds to a distinct deformation of the zinc blende lattice.

formation of two new bonds for each Ga (As) atom with a pair of next-nearest neighbors, both of which are at a distance of 0.75 times the lattice constants along one of the conventional fcc unit cell vectors of the zinc blende lattice. As there are six such distinct pairs, the transformation can proceed through as many different paths. Each of these paths corresponds to a unique deformation (strain) relative to the original zinc blende lattice and can result in a different orientation for the rocksalt phase.

The one-to-one correspondence between deformation and bond formation has been used to conveniently identify nucleation and growth of different rocksalt domains. The domains may be defined based on the deformation, but are identified based on the new bonds formed during transformation. This circumvents ambiguity in the final absolute domain orientation caused by rotations that occur to maintain the connectivity of the nanocrystal. A cross section of the nanocrystal from the simulation monitoring the transformation continuously is shown in Fig. 4. Domains nucleate on the surface and grow inwards with increasing pressure, consistent with the bond-angle distributions (Fig. 2).

Figure 5(a) shows a slice of the system corresponding to the cross-section in Fig. 4(c). A grain boundary can be identified between domains labeled 1 and 3, whereas this does not appear to be the case between domains labelled 2 and 3. The presence or absence of grain boundaries between any two domains that have undergone different strains can be understood from a geometrical construction. Beginning with a spherical nanocrystal with zinc blende structure, the domains are constructed by applying two different linear transformations and a corresponding relative shift between the Ga and As sublattices. The boundary between the two domains is restricted to a plane, and the ori-

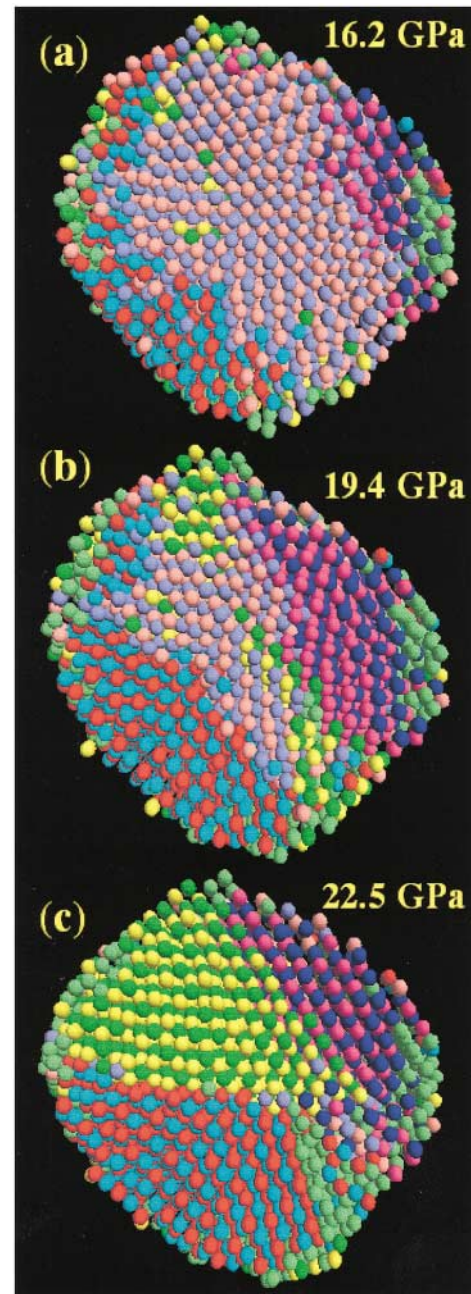


FIG. 4 (color). Formation and growth of rocksalt domains. Domains in a cross section of the spherical nanocrystal of diameter 60 Å are shown as pressure is increased linearly in time. Dull (blue/pink) colors identify atoms in regions with zinc blende structure; bright colors identify atoms in regions with rocksalt structure. Three rocksalt domains are distinguished with atoms colored red/cyan (number 1), blue/magenta (number 2), and green/yellow (number 3). The light green color identifies regions with very small/indistinct domains. (a) At 16.2 GPa domains, 1 and 2 have already nucleated on the surface. (b) At 19.4 GPa domains, 1 and 2 have grown inwards. Domain 3 nucleates on the surface of the nanocrystal. (c) At 22.5 GPa, the transformation is completed with the three domains growing into the center of the nanocrystal.

entation of the planar boundary between the two domains is determined from the condition that the in-plane strains

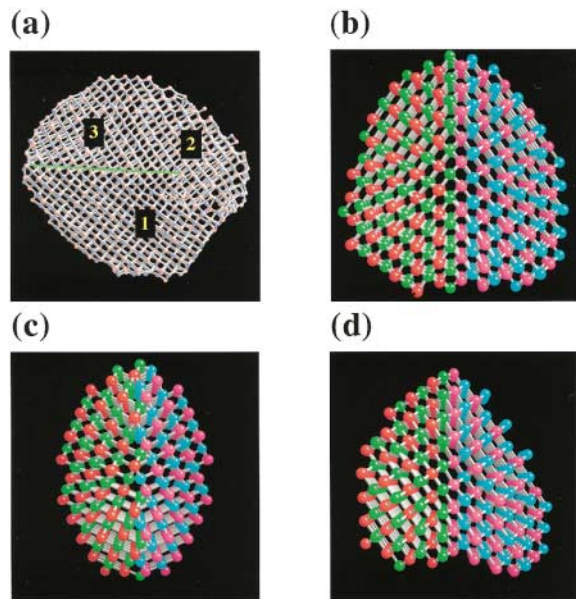


FIG. 5 (color). Strain and orientation of domains in the nanocrystal. (a) 8 Å slice of the nanocrystal (diameter 60 Å) corresponding to the cross section in Fig. 4(c). Strain domains 1 and 3 are separated by a grain boundary that is identified by the green line, whereas domains 2 and 3 are not. (b)–(d) are perspective views of a spherical nanocrystal of diameter 30 Å that has been geometrically transformed differently in the red/green and cyan/magenta regions. Configurations (b) and (c) show a grain boundary as the two regions after transformation have inequivalent orientation. Configuration (d) does not show a grain boundary as the transformed regions have the same orientation. Even in the absence of a grain boundary the nonellipsoidal shape of the transformed nanocrystal distinguishes this case from that corresponding to uniform strain. In (a) the boundary between strain domains 1 and 3 can be identified to be of the type shown in (b). Domains 2 and 3 do not show a clear distinction in orientation: the boundary between them therefore corresponds to the type shown in (d).

for the linear transformations be equal. Relative rotation of the planar boundary due to the two transformations is also set to zero. Hence, by construction, this procedure can lead only to tilt grain boundaries (Fig. 5). Considering the symmetries of a fcc lattice, this procedure results in only three distinct configurations. Two of these configurations [Figs. 5(b) and 5(c)] are grain boundaries, since the orientation of the resulting rocksalt domains is different. The third [Fig. 5(d)] is not a grain boundary because the resulting rocksalt domains have the same orientation. However, it is different from the case of a uniform strain since the resulting shape of an initially spherical nanocrystal is not ellipsoidal. Two of these configurations [Figs. 5(b) and 5(d)] are indeed observed in the simulation results [Figs. 4(c) and 5(a)].

The results of this parallel molecular-dynamics study on structural transformation in GaAs nanocrystals under pressure show that the transformation from the zinc blende phase to the rocksalt phase begins from the surface and proceeds inwards with increasing pressure. The transformed

GaAs nanocrystals have grains of the rocksalt phase separated by grain boundaries. Considering the atomic mechanism of the zinc blende to rocksalt transformation, this implies nonuniform deformation of the nanocrystals under transformation. Even in the absence of grain boundaries, different regions of the nanocrystal may have undergone inequivalent deformation relative to the original zinc blende lattice. Such cases can nevertheless be distinguished from that corresponding to uniform deformation as the transformed nanocrystal would have a nonellipsoidal shape. A study of the dependence of the structural transformation on the size and shape of nanocrystals is in progress. This is of interest as experimental observations on different materials [7–9,24] show opposite trends in the variation of the transition pressure with nanocrystal size.

This work has been supported by NSF, DOE, AFOSR, USC-LSU MURI, and NASA. The authors thank Shuji Ogata and Antonio De Silva for useful discussions, and Timothy Campbell for help with visualization.

-
- [1] S. T. Weir *et al.*, Phys. Rev. B **39**, 1280 (1989).
 - [2] J. M. Besson *et al.*, Phys. Rev. B **44**, 4214 (1991).
 - [3] S. Froyen and M. L. Cohen, Phys. Rev. B **28**, 3258 (1983).
 - [4] S. B. Zhang and M. L. Cohen, Phys. Rev. B **35**, 7604 (1987).
 - [5] K. Kunc and R. M. Martin, Phys. Rev. B **24**, 2311 (1981).
 - [6] M. Haase and A. P. Alivisatos, J. Phys. Chem. **96**, 6756 (1992).
 - [7] S. H. Tolbert and A. P. Alivisatos, J. Chem. Phys. **102**, 4642 (1995).
 - [8] S. H. Tolbert *et al.*, Phys. Rev. Lett. **76**, 4384 (1996).
 - [9] J. N. Wickham, A. B. Herhold, and A. P. Alivisatos, Phys. Rev. Lett. **84**, 923 (2000).
 - [10] N. Binggeli and J. R. Chelikowsky, Nature (London) **353**, 344 (1991).
 - [11] R. M. Wentzcovitch *et al.*, Phys. Rev. Lett. **80**, 2149 (1998).
 - [12] R. Martonak, C. Molteni, and M. Parrinello, Phys. Rev. Lett. **84**, 682 (2000).
 - [13] F. Shimojo *et al.*, Phys. Rev. Lett. **84**, 3338 (2000).
 - [14] J. P. Rino *et al.*, (to be published).
 - [15] G. J. Martyna, D. J. Tobias, and M. L. Klein, J. Chem. Phys. **101**, 4177 (1992).
 - [16] M. Tuckerman, B. J. Berne, and G. J. Martyna, J. Chem. Phys. **97**, 1990 (1992).
 - [17] G. J. Martyna *et al.*, Mol. Phys. **87**, 1117 (1996).
 - [18] M. Z. Bazant, E. Kaxiras, and J. F. Justo, Phys. Rev. B **56**, 8542 (1997).
 - [19] I. Ebbsjö *et al.*, J. Appl. Phys. **87**, 7708 (2000).
 - [20] D. Strauch and B. Dorner, J. Phys. Condens. Matter **2**, 1457 (1990).
 - [21] D. Udron *et al.*, J. Non-Cryst. Solids **137–138**, 131 (1991).
 - [22] J. K. Johnson, J. A. Zollweg, and K. E. Gubbins, Mol. Phys. **78**, 591 (1993).
 - [23] J. P. Rino *et al.*, Phys. Rev. B **47**, 3053 (1993).
 - [24] J. Z. Jiang *et al.*, Europhys. Lett. **44**, 620 (1998).